

## Scattering of cold $^4\text{He}$ on $^4\text{He}^{6,7}\text{Li}$ and $^4\text{He}^{23}\text{Na}$ molecules

M. A. Shalchi,<sup>1</sup> A. Delfino,<sup>2</sup> T. Frederico,<sup>3</sup> and Lauro Tomio<sup>1,3</sup>

<sup>1</sup>*Instituto de Física Teórica, Universidade Estadual Paulista, 01405-900 São Paulo, Brazil*

<sup>2</sup>*Instituto de Física, Universidade Federal Fluminense, 24210-310 Niterói, Rio de Janeiro, Brazil*

<sup>3</sup>*Instituto Tecnológico de Aeronáutica, DCTA, 12228-900 São José dos Campos, Brazil*



(Received 8 August 2018; published 24 September 2018)

We predict  $s$ -wave elastic cross-sections  $\sigma$  for low-energy atom-molecule collisions with kinetic energies up to 40 mK for the  $^4\text{He}$  collision with weakly bound diatomic molecules formed by  $^4\text{He}$  with  $^7\text{Li}$ ,  $^6\text{Li}$ , and  $^{23}\text{Na}$ . Our scattering calculations are performed by using diatomic and triatomic molecular binding energies obtained from several available realistic models as input in a renormalized zero-range model as well as a finite-range one-term separable potential in order to quantify the relevance of range corrections to our predictions. Of particular relevance for possible experimental realization, we show the occurrence of a zero in  $\sigma$  for the collision of cold  $^4\text{He}$  on a  $^4\text{He}^{23}\text{Na}$  molecule below 20 mK. Also our results for the elastic collision  $^4\text{He}$  on  $^4\text{He}^{6,7}\text{Li}$  molecules suggest that  $\sigma$  varies considerably for the realistic models studied. As the chosen molecules are weakly bound and the scattering energies are very low, our results are interpreted on the light of the Efimov physics, which explains the model independence and robustness of our predictions despite some sensitivity on the potential range.

DOI: [10.1103/PhysRevA.98.032705](https://doi.org/10.1103/PhysRevA.98.032705)

### I. INTRODUCTION

The Efimov effect [1] is a peculiar pure quantum-mechanical effect, expected to occur in three-body quantum systems, manifested by an increasing number of three-body bound states when the absolute value of the scattering length of a two-body subsystem is approaching infinity. This effect has a long tradition of studies in the nuclear physics context, sometimes being mentioned as the *Thomas-Efimov* effect [2], considering its relation to another property of the three-body Schrödinger formalism noticed by Thomas [3] in 1935 when investigating the origin of the nuclear forces between nucleons. By considering a nonrelativistic two-boson interaction supporting one bound state, he observed that the three-body ground-state will collapse to  $-\infty$  in the limit when the range of the interaction is zero. This observation was essential for the first conclusions on the range of about 1 fm of the nuclear forces. Besides the fact that the initial investigations on Efimov states in nuclear physics have been limited to theoretical approaches not experimentally realizable (as the two-body interaction is fixed), we should note some theoretical efforts in given evidence that some well-known states could eventually be considered as manifestations of Efimov states by considering the behavior of such states when varying the potential parameters such that the two-body interaction is driven to the unitary limit. In particular, this is the case of the original proposal that the virtual state of the  $s$ -wave spin doublet trinucleon system is an Efimov state [4]. The interest in verifying manifestations of Efimov physics in nuclear physics came much later with the discovery of exotic nuclei [5] having two neutrons far apart from a core [6–8]. Since then, extensive investigations on universal aspects of light halo nuclei are available in the context of Efimov physics, which can be traced by several reviews. For that,

we can mention Refs. [9–13] in which the updated review on the halo-nuclei description of Ref. [13] is exploring the effective field-theory approach. In view of the limitations to observe indications of the Efimov effect coming from nuclear physics aspects, most of the initial theoretical studies on Efimov states have been considered three-atom systems by using realistic interatomic interactions [14–19]. The trimer of  $^4\text{He}$  due to the very weak binding of the corresponding dimer was long-time predicted in 1977 to present an Efimov state in Ref. [14] on the basis of a three-body calculation in momentum space using Faddeev formalism. Their investigation was followed by several other related works performed in the same period [15,16]. Later on, in another independent work within the Faddeev scheme, Cornelius and Glöckle [17] confirmed the existence of two bound states for the  $^4\text{He}$  trimer with the weakly bound excited state having the property of an Efimov state. The existence of the weakly bound excited state in helium, established in Ref. [17], also proved to be a good test for the predicting power of the scaling approach presented in Ref. [19] (essentially the same result is obtained). The search for Efimov states in such a system [20–28] has been motivated by the remarkable low binding energy of the  $^4\text{He}$  dimer:  $B_{^4\text{He}_2} = 1.31$  millikelvins (mK) [29]. Finally, in 2015, in Ref. [30], the experimental observation of this long-time predicted Efimov state was reported. The experimental success in verifying such a long-time theoretical prediction together with the results of previous experimental investigations of Efimov physics in cold atom laboratories [31], which are extended to mixed atomic-molecular combinations [32], became highly motivating for deeper theoretical studies with single or mixed atomic species [33–38]. Quite remarkable are the advances in the laboratory techniques such that one can even consider the possibility to alter the two-body interaction by using Feshbach resonance mechanisms (originally

proposed in the nuclear physics context) [39]. In ultracold atom experiments, the possibility for changing the two-body scattering length was shown that can alter in an essential way the balance between the nonlinear first few terms of the mean-field description which is modeling the atomic Bose-Einstein condensation [40].

In the present paper, by following previous studies on triatomic molecules involving the helium atom, in particular, considering available results reported in Ref. [41] for realistic interactions, we are studying the cold atom-dimer elastic collision. Our paper is focused on the cases where the three-body system is composed of a mixture with  $^4\text{He}$  and another atomic species chosen as being  $^6\text{Li}$ ,  $^7\text{Li}$ , and  $^{23}\text{Na}$ . In all the cases, we assume  $^4\text{He}$  as the colliding particle with the dimer formed by the remaining two-body subsystem. For the present paper, we consider the Faddeev formalism using finite-range (FR) separable two-body interactions as well as the renormalized zero-range (ZR) model [8]. The main observables that we are concerned with as relevant for possible experimental investigations are the  $s$ -wave phase shifts and the elastic  $s$ -wave cross section for different colliding and dimer energies. In order to help us with the analysis of the  $s$ -wave elastic-scattering amplitude, the results for the absorption parameter are also presented in some relevant cases.

As we are concerned with relatively low kinetic colliding energies with the lowest partial wave being more relevant for the Efimov physics, we focus our paper on the  $s$ -wave contribution to the total cross section. The corresponding contributions due to higher partial waves, such as from  $p$  and  $d$  waves, which should appear for increasing kinetic energies, are left to be explored in a future related investigation. However, as will be shown here, the more interesting outcome is verified for kinetic energies where the  $s$  wave is expected to dominate.

In the next section, we present the formalism. The main results with a corresponding discussion are given in Sec. III. In Sec. IV we give our final remarks and conclusions.

## II. FADDEEV THREE-BODY FORMALISM

In the present section, we fix our notation and include the standard formalism for the elastic-scattering amplitude of a particle  $\alpha$  colliding to a dimer ( $\alpha\beta$ ), which is formed by the same particle  $\alpha$  with another particle  $\beta$ . For convenience, as explained in our Introduction, we choose  $\alpha$  as the  $^4\text{He}$  atom with  $\beta$  being  $^7\text{Li}$ ,  $^6\text{Li}$ , or  $^{23}\text{Na}$ . In the following formalism, we are always considering that the three-body system ( $\alpha\alpha\beta$ ) as well as the subsystems ( $\alpha\beta$ ) and ( $\alpha\alpha$ ) are bound such that we can take advantage of the corresponding available data as inputs coming from different realistic models as well as from experimental considerations. Therefore, everywhere along this presentation we are assuming as fixed the  $^4\text{He}_2$  binding energy and corresponding scattering length such that  $E_{\alpha\alpha} = -B_{\alpha\alpha} = -1.31$  mK and  $a_{\alpha\alpha} = 100$  Å. The other input binding energies are obtained from specific models, which will be discussed. In particular, we should note the good agreement among most of the realistic models on the other dimer binding energies  $\alpha\beta$  such that the discrepancies coming from the model results are mainly verified for the respective three-body energies.

In the formalism, following Ref. [42], we assume units such that  $\hbar = 1$  (with energies given in mK) with  $m \equiv m_\alpha = m_{^4\text{He}}$  and a mass ratio which is defined by  $A \equiv m_\beta/m_\alpha$  such that  $\mu_{\alpha\alpha} = m/2$  and  $\mu_{\alpha\beta} = Am/(A+1)$  are the reduced masses for the  $\alpha\alpha$  and  $\alpha\beta$  subsystems, respectively, with the corresponding three-body reduced masses given by  $\mu_{\alpha(\alpha\beta)} = m(A+1)/(A+2)$  for  $\alpha - (\alpha\beta)$ ; and  $\mu_{\beta(\alpha\alpha)} = m(2A)/(A+2)$  for  $\beta - (\alpha\alpha)$ . The bound-state energies for the two- and three-body systems are given by  $E_{\alpha\alpha} \equiv -B_{\alpha\alpha}$ ,  $E_{\alpha\beta} \equiv -B_{\alpha\beta}$ , and  $E_3 \equiv -B_3$ , respectively, with the energy of the  $s$ -wave elastic colliding particle given by  $E_k$ . In the following, we first recover the bound-state three-body formalism, restricted to the  $s$ -wave case when all the subsystems being bound. Next, by introducing the appropriate boundary conditions we extend the formalism to atom-dimer collision.

### A. Three-body $\alpha\alpha\beta$ bound state

The bound-state coupled equation for separable potentials is usually written in terms of the spectator functions for the particles  $\alpha$  and  $\beta$

$$\begin{aligned}\chi_\alpha(q) &= \tau_\alpha(q; E_3) \int_0^\infty dk k^2 [K_2(q, k; E_3) \chi_\alpha(k) \\ &\quad + K_1(q, k; E_3) \chi_\beta(k)], \\ \chi_\beta(q) &= 2\tau_\beta(q; E_3) \int_0^\infty dk k^2 K_1(k, q; E_3) \chi_\alpha(k),\end{aligned}\quad (1)$$

where  $\chi_\alpha(q) \equiv \chi_\alpha(q; E_3)$  and  $\chi_\beta(q) \equiv \chi_\beta(q; E_3)$ .  $\tau_\alpha$  and  $\tau_\beta$  are the respective two-body  $t$  matrices for the  $\alpha\beta$  and  $\alpha\alpha$  subsystems with  $K_1$  and  $K_2$  being the appropriate kernels, which will be explicitly given in the following according to the kind of form factors one considers for the two-body interactions.

By considering the definitions,

$$\frac{k_\alpha^2}{2\mu_{\alpha(\alpha\beta)}} \equiv E_3 - E_{\alpha\beta}, \quad \frac{k_\beta^2}{2\mu_{\beta(\alpha\alpha)}} \equiv E_3 - E_{\alpha\alpha}, \quad (2)$$

with  $j = \alpha, \beta$ ,  $\tau_j$ ,  $\chi_j$  the coupled Eq. (1) can be conveniently redefined. As both subsystems are bound, we have

$$\tau_j(q; E_3) \equiv \frac{\bar{\tau}_j(q; E_3)}{q^2 + |k_j^2|}, \quad \chi_j(q) \equiv \frac{h_j(q; E_3)}{q^2 + |k_j^2|}, \quad (3)$$

with

$$\begin{aligned}h_\alpha(q; E_3) &= \bar{\tau}_\alpha(q; E_3) \int_0^\infty dk k^2 \left[ K_2(q, k; E_3) \frac{h_\alpha(k; E_3)}{(k^2 + |k_\alpha^2|)} \right. \\ &\quad \left. \times K_1(q, k; E_3) \frac{h_\beta(k; E_3)}{(k^2 + |k_\beta^2|)} \right], \\ h_\beta(q; E_3) &= \bar{\tau}_\beta(q; E_3) \int_0^\infty dk k^2 K_1(k, q; E_3) \frac{h_\alpha(k; E_3)}{(k^2 + |k_\alpha^2|)}.\end{aligned}\quad (4)$$

The expressions for  $\bar{\tau}_j$  and kernels  $K_{1,2}$  are given in the following Sec. II C by considering the specific potential models that we are using.

### B. Atom-dimer collision

For the scattering of a particle  $\alpha$  by the  $\alpha\beta$  bound subsystem, we should first redefine the expression for  $\tau_\alpha$  given in Eq. (3) (considering that  $k_\alpha^2 > 0$ ) such that  $\tau_\alpha(q; E_3) \equiv \bar{\tau}_\alpha(q; E_3)/(q^2 - k_\alpha^2 - i\epsilon)$ . Next, the formalism is extended to obtain the scattering amplitude by introducing the required boundary condition. For the  $s$  wave, this condition is given by

$$\chi_\alpha(q) \equiv 2\pi^2 \frac{\delta(q - k_\alpha)}{q^2} + 4\pi \frac{h_\alpha(q; E_3)}{q^2 - k_\alpha^2 - i\epsilon}, \quad (5)$$

where  $k_\alpha$  is given by Eq. (2) with  $E_3 > 0$  in this case. So, the coupled equations (4) are replaced by

$$h_\alpha(q; E_3) = \bar{\tau}_\alpha(q; E_3) \left\{ \frac{\pi}{2} K_2(q, k_\alpha; E_3) + \int_0^\infty dk k^2 \right. \\ \left. \times \left[ K_2(q, k; E_3) \frac{h_\alpha(k; E_3)}{(k^2 - k_\alpha^2 - i\epsilon)} \right. \right. \\ \left. \left. + K_1(q, k; E_3) \frac{h_\beta(k; E_3)}{q^2 - k_\beta^2} \right] \right\}, \quad (6)$$

$$h_\beta(q; E_3) = \bar{\tau}_\beta(q; E_3) \left\{ \frac{\pi}{2} K_1(k_\alpha, q; E_3) \right. \\ \left. + \int_0^\infty dk k^2 K_1(k, q; E_3) \frac{h_\alpha(k; E_3)}{(k^2 - k_\alpha^2 - i\epsilon)} \right\}. \quad (7)$$

### C. Zero-range and finite-range interactions with corresponding kernels

When using zero-range interactions, a momentum cutoff is required to regularize the formalism within a renormalization procedure. For that, in the kernels a subtraction procedure is used with a regularizing momentum parameter  $\mu$  such that the kernels  $K_{1,2}$  and  $\bar{\tau}_j$  used in the formalism are given by

$$K_{i=1,2}(q, k; E_3) \equiv G_i(q, k; E_3) - G_i(q, k, -\mu^2), \\ G_1(q, k; E_3) = \int_{-1}^1 dx \left[ E_3 + i\epsilon - \frac{q^2}{m} - \frac{k^2}{2\mu_{\alpha\beta}} - \frac{kqx}{m} \right]^{-1} \\ G_2(q, k; E_3) = \int_{-1}^1 dx \left[ E_3 + i\epsilon - \frac{q^2 + k^2}{2\mu_{\alpha\beta}} - \frac{kqx}{Am} \right]^{-1}, \quad (8)$$

$$\bar{\tau}_\alpha(q; E_3) \equiv \frac{\mu_{\alpha(\alpha\beta)}}{2\pi\mu_{\alpha\beta}^2} [\kappa_{\alpha\beta} + \kappa_{3,\alpha\beta}(E_3)], \quad (9)$$

$$\bar{\tau}_\beta(q; E_3) \equiv \frac{\mu_{\beta(\alpha\alpha)}}{2\pi\mu_{\alpha\alpha}^2} [\kappa_{\alpha\alpha} + \kappa_{3,\alpha\alpha}(E_3)], \quad (10)$$

where

$$\kappa_{\alpha\alpha} \equiv \sqrt{-2\mu_{\alpha\alpha} E_{\alpha\alpha}}, \\ \kappa_{\alpha\beta} \equiv \sqrt{-2\mu_{\alpha\beta} E_{\alpha\beta}}, \\ \kappa_{3\alpha\alpha}(E_3) \equiv \sqrt{-2\mu_{\alpha\alpha} \left[ E_3 - \frac{q^2}{2\mu_{\beta(\alpha\alpha)}} \right]}, \\ \kappa_{3\alpha\beta}(E_3) \equiv \sqrt{-2\mu_{\alpha\beta} \left[ E_3 - \frac{q^2}{2\mu_{\alpha(\alpha\beta)}} \right]}. \quad (11)$$

For finite-range interaction, we assume a rank-one separable Yamaguchi potential, given by

$$V_{ij}(p, p') = \lambda_{ij} \left( \frac{1}{p^2 + \gamma_{ij}^2} \right) \left( \frac{1}{p'^2 + \gamma_{ij}^2} \right), \quad (12)$$

where  $ij = \alpha\alpha$  or  $\alpha\beta$ , respectively, for the  $\alpha\alpha$  or  $\alpha\beta$  two-body subsystems.  $\lambda_{ij}$  and  $\gamma_{ij}$  refer to the strength and range  $r_{ij}$  of the respective two-body interactions. As in the present approach we consider only bound (negative) two-body subsystems  $E_{ij} = -B_{ij}$ , the corresponding relations for the strengths and ranges are given by

$$\lambda_{ij}^{-1} = \frac{-2\pi\mu_{ij}}{\gamma_{ij}(\gamma_{ij} + \kappa_{ij})^2}, \quad r_{ij} = \frac{1}{\gamma_{ij}} + \frac{2\gamma_{ij}}{(\gamma_{ij} + \kappa_{ij})^2}. \quad (13)$$

In this case,  $K_{1,2}$  and  $\bar{\tau}_j$  are given by the following:

$$K_1(q, k; E_3) = \int_{-1}^1 dx \left[ q^2 + \frac{k^2}{4} + qkx + \gamma_{\alpha\alpha}^2 \right]^{-1} \\ \times \left[ k^2 + \frac{q^2 A^2}{(A+1)^2} + \frac{2qkAx}{(A+1)} + \gamma_{\alpha\beta}^2 \right]^{-1} \\ \times \left[ E_3 + i\epsilon - \frac{q^2}{m} - \frac{k^2}{2\mu_{\alpha\beta}} - \frac{qkx}{m} \right]^{-1}, \quad (14)$$

$$K_2(q, k; E_3) = \int_{-1}^1 dx \left[ k^2 + \frac{q^2}{(A+1)^2} + \frac{2qkx}{(A+1)} + \gamma_{\alpha\beta}^2 \right]^{-1} \\ \times \left[ q^2 + \frac{k^2}{(A+1)^2} + \frac{2qkx}{(A+1)} + \gamma_{\alpha\beta}^2 \right]^{-1} \\ \times \left[ E_3 + i\epsilon - \frac{(q^2 + k^2)}{2\mu_{\alpha\beta}} - \frac{qkx}{Am} \right]^{-1}, \quad (15)$$

$$\bar{\tau}_\alpha(q; E_3) \equiv \frac{\mu_{\alpha(\alpha\beta)}}{\pi\mu_{\alpha\beta}^2} \left[ \frac{\gamma_{\alpha\beta}(\gamma_{\alpha\beta} + \kappa_{\alpha\beta})^2}{2\gamma_{\alpha\beta} + \kappa_{3\alpha\beta}(E_3) + \kappa_{\alpha\beta}} \right. \\ \left. \times [\gamma_{\alpha\beta} + \kappa_{3\alpha\beta}(E_3)]^2 [\kappa_{\alpha\beta} + \kappa_{3\alpha\beta}(E_3)] \right], \quad (16)$$

$$\bar{\tau}_\beta(q; E_3) \equiv \frac{\mu_{\beta(\alpha\alpha)}}{\pi\mu_{\alpha\alpha}^2} \left[ \frac{\gamma_{\alpha\alpha}(\gamma_{\alpha\alpha} + \kappa_{\alpha\alpha})^2}{2\gamma_{\alpha\alpha} + \kappa_{3\alpha\alpha}(E_3) + \kappa_{\alpha\alpha}} \right. \\ \left. \times [\gamma_{\alpha\alpha} + \kappa_{3\alpha\alpha}(E_3)]^2 [\kappa_{\alpha\alpha} + \kappa_{3\alpha\alpha}(E_3)] \right]. \quad (17)$$

In our approach, the parameters of the separable interactions are fixed by the corresponding bound-state energies as well as by the effective ranges (when considering finite-range interactions).

Finally, the scattering observables,  $s$ -wave phase-shift  $\delta_0$ , cross-section  $\sigma$ , and absorption parameter  $\eta$  are obtained by using the on-shell scattering amplitude  $h_\alpha(k; E_3)$ , considering that

$$h_\alpha(k; E_3) = \frac{S_\alpha - 1}{2ik}, \quad (18)$$

$$S_\alpha = \eta e^{2i\delta_0}, \quad \frac{d\sigma}{d\Omega} = |h_\alpha(k; E_3)|^2, \quad (19)$$

where  $S_\alpha$  is the scattering matrix for the elastic  $s$ -wave channel and  $\eta \leq 1$  is the absorption parameter.

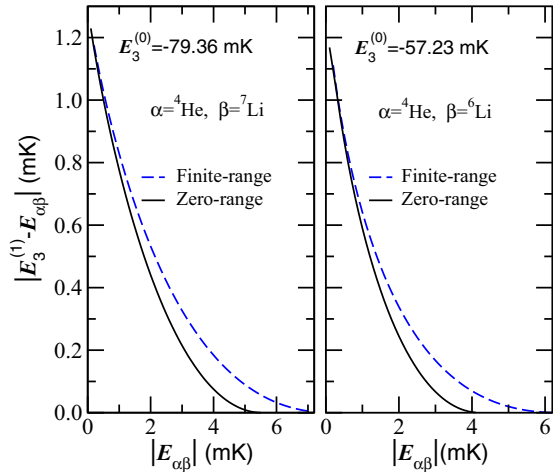


FIG. 1. For the  ${}^4\text{He}_2 {}^7\text{Li}$  (left frame) and  ${}^4\text{He}_2 {}^6\text{Li}$  (right frame) three-body systems with  $\alpha \equiv {}^4\text{He}$  and  $\beta \equiv {}^7\text{Li}$ ,  ${}^6\text{Li}$ , respectively, we show the behavior of the corresponding three-body excited states  $E_3^{(1)}$ , which are represented by the absolute value of  $E_3^{(1)} - E_{\alpha\beta}$  in terms of the dimer binding energies  $E_{\alpha\beta}$ . As indicated inside the frames, the results are obtained by using zero-range and finite-range two-body interactions with the given values for  $E_3^{(0)}$ . The  ${}^4\text{He}_2$  bound state in both cases is fixed to  $B_{\alpha\alpha} = |E_{\alpha\alpha}| = 1.31$  mK.

### III. RESULTS

In this section we present our main results and analysis for the scattering of an atom of  ${}^4\text{He}$  colliding with a weakly bound diatomic molecule composed of  ${}^4\text{He}$  with  ${}^6,{}^7\text{Li}$  or  ${}^{23}\text{Na}$ . In this regard, by considering that the two-body subsystems in this paper are weakly bound, the relevant low-energy observables that we focus on are the  $s$ -wave cross sections, which are directly related to the  $s$ -wave phase-shifts  $\delta_0$ , and the corresponding absorption parameter. For that, we use different two-body interactions, namely, the renormalized zero-range model and a finite-range model given by the one-term separable Yamaguchi potential. In both cases, we assume as inputs the available binding energies from different realistic model calculations. In the case of the ZR model, the inputs are introduced in the renormalization procedure; whereas, for the finite-range case, the inputs are used to adjust the parameters (range and strength) of the Yamaguchi potential.

#### A. ${}^4\text{He}_2 {}^7,{}^6\text{Li}$ Efimov molecules

Before moving to the main focus of this presentation on the atom-molecule scattering, we study the relevance of the range in the formation of excited Efimov triatomic states by comparing results obtained with both potential models in situations where such states are expected to exist. These are the cases of  ${}^4\text{He}_2 {}^7\text{Li}$  and  ${}^4\text{He}_2 {}^6\text{Li}$  where we fix the well-known  ${}^4\text{He}_2$  dimer energy  $B_{\alpha\alpha} = 1.31$  mK together with the corresponding ground-state three-body energies given in Ref. [41]:  $E_3^{(0)} = -79.36$  mK for  ${}^4\text{He}_2 {}^7\text{Li}$  and  $-57.23$  mK for  ${}^4\text{He}_2 {}^6\text{Li}$ . Our results for the excited three-body bound-state energies (reduced by the corresponding two-body bound-state energies), obtained by the ZR and Yamaguchi models, are shown in the two frames of Fig. 1 as a function of the two-body binding energies.

As shown in the left frame of Fig. 1, the finite-range Yamaguchi potential, which reproduces the given  ${}^4\text{He}_2$  dimer and the  ${}^4\text{He}_2 {}^7\text{Li}$  ground-state binding energies, will allow an excited Efimov state if we have a  ${}^4\text{He} {}^7\text{Li}$  dimer bound with a binding energy less than  $\sim 7$  mK. Correspondingly, as shown in the right frame, the upper limit of the  ${}^4\text{He} {}^6\text{Li}$  dimer energy to produce an excited three-body state is  $\sim 6$  mK when using the FR Yamaguchi potential. For the zero-range model, the upper limit for the binding energy of the dimer to allow an excited state is  $\sim 5.5$  mK for  ${}^4\text{He}_2 {}^7\text{Li}$  and being  $\sim 4.1$  mK for  ${}^4\text{He}_2 {}^6\text{Li}$ .

In Fig. 1 are shown results for particular examples, considering the given binding energies, of the universal scaling behavior theoretically found for weakly bound triatomic states when considering two-species atomic systems close to the Efimov limit where the sizes of the ground-state trimer and dimers are much larger than the interaction range. Such a situation is associated with a large probability of occupation of the classically forbidden region dominated by the dynamics of a free Hamiltonian, scale invariant and model independent. The correlation between the excited triatomic binding energy and the ground state comes from the breaking of the continuous scale invariance to a discrete one, which translates in a universal scaling function as the limit cycle of the discrete Efimov scaling [19,43] when the range of the interaction is driven towards zero (see, e.g., the reviews [12,13]).

The interaction range allows more room for the formation of the Efimov state, namely, the critical value of the  ${}^4\text{He} {}^6,{}^7\text{Li}$  molecular binding can be somewhat larger as one can see in Fig. 1 through the comparison between the ZR and the Yamaguchi potential results. The effective range expansion says that the scattering length for a given dimer binding energy increases with the effective range as

$$a_{\alpha\beta} \approx \left( \kappa_{\alpha\beta} - \frac{1}{2} r_{\alpha\beta} \kappa_{\alpha\beta}^2 \right)^{-1} \approx \kappa_{\alpha\beta}^{-1} + \frac{1}{2} r_{\alpha\beta} \kappa_{\alpha\beta}, \quad (20)$$

which shows that the cut of the tail of the attractive Efimov long-range potential should increase with the effective range. Therefore, the formation of the large triatomic excited state is favored when the range of the short interaction increases in the situation where ground-state energy is kept fixed.

The scaling plot shown in the figure was first derived and presented in Fig. 2 of Ref. [19] for trimers composed of identical bosonic atoms. A general study of the universal three-particle behavior with two kinds of particles was previously presented in Ref. [8]. We complement the plots shown in Fig. 1 and Table I where realistic values for the two-body subsystem (given in the second and third columns) and for the three-body ground-state energy (fourth column) are shown from Ref. [18] (also considered in Ref. [23]) and Ref. [41]. In the second block of the table we have the corresponding predicted three-body excited states with the values obtained in Ref. [41] given in the fifth column. Our corresponding results when using the two- and three-body binding energies given in the second and fourth columns are presented in the sixth and seventh columns by using the zero-range and finite-range approaches. In all these cases, the binding energy of  ${}^4\text{He}$  is  $B_{\alpha\alpha} = 1.31$  mK with the corresponding scattering length being  $a_{\alpha\alpha} = 100$  Å.

TABLE I. For the three-body molecular systems identified in the first column, given the two-body energies and scattering lengths in the second and third columns and the three-body ground-state energies in the fourth column as given in Ref. [41], we have the first excited bound-state energies in the fifth to seventh columns. In the fifth column the results are from Ref. [41]. Our results for the excited states using ZR and FR one-term Yamaguchi interactions are shown in the sixth and seventh columns. In our notation,  $\alpha$  and  $\beta$  are identifying, respectively,  $^4\text{He}$  and the other atomic species ( $^6,^7\text{Li}$ ,  $^{23}\text{Na}$ ). In all the cases, for the  $^4\text{He}$  dimer, we have the well-known value of  $B_{\alpha\alpha} = 1.31$  with the scattering length being  $a_{\alpha\alpha} = 100 \text{ \AA}$ .

$\alpha\alpha\beta$	$B_{\alpha\beta}$	$a_{\alpha\beta}$	$B_3^{(0)}$	$B_{\alpha\alpha\beta}^{(1)}$	$B_{3(\text{ZR})}^{(1)}$	$B_{3(\text{FR})}^{(1)}$
$\alpha = ^4\text{He}$	(mK)	(\AA)	(mK)	(mK)	(mK)	(mK)
$\beta = ^7\text{Li}$	5.622	48.84	79.36	5.642		5.672
$\beta = ^6\text{Li}$	1.515	100	57.23	1.937	1.901	1.977

We have to add that the effect of the range in the case of the molecule  $^4\text{He}_2\ ^7\text{Li}$  with the parameters from Ref. [41] and given in Table I allows one Efimov excited state with the binding energy of 5.7 mK. In this case as the binding energy of the  $^4\text{He}_2\ ^7\text{Li}$  molecule is comparatively high with respect to the ground-state energy, the range gives the crucial contribution to increase the scattering length and the cut in the long-range effective Efimov potential such that the excited state is barely bound. This state heals over quite incredibly long distances, namely, of about 800–900 \AA. If that comes true, the binding energy of these excited states will be a sensitive indirect measure of the interaction range. The other lithium isotope  $^6\text{Li}$  forms a weakly bound molecule with  $^4\text{He}$ , and there is little effect of the interaction range in the  $^4\text{He}_2\ ^6\text{Li}$  Efimov excited state.

### B. Elastic scattering of $^4\text{He}$ on $^4\text{He}$ , $^6,^7\text{Li}$ , $^{23}\text{Na}$

In order to pursue our aim in studying the atom-dimer systems with  $\alpha \equiv ^4\text{He}$  as the projectile and dimers  $\alpha\beta$ , where  $\beta \equiv ^7\text{Li}$ ,  $^6\text{Li}$ , and  $^{23}\text{Na}$ , next we provide Tables II and III, which we have considered to calculate the corresponding elastic atom-dimer  $s$ -wave cross sections.

TABLE II. Available two- and three-body ground-state binding energies (absolute values, given in millikelvins) for the three atomic systems given by  $\alpha = ^4\text{He}$ ,  $\beta = ^7\text{Li}$ ,  $^6\text{Li}$ , and  $^{23}\text{Na}$  from different model potentials. (a1) is from Ref. [41]; (a2) is from Ref. [18]; (a3), (a4), and (a6) are from Ref. [25]; (a5) is from Ref. [24]; (a7) is from Ref. [27]; (a8) is from Ref. [28]. These data are being considered as inputs in our numerical approach on the atom-dimer collision.

	(a1)	(a2)	(a3)	(a4)	(a5)	(a6)	(a7)	(a8)
$^4\text{He}\ ^7\text{Li}$	5.622	2.16	5.621	5.621	2.81	2.81	5.355	5.621
$^4\text{He}\ ^6\text{Li}$	1.515	0.12			0.33			1.515
$^4\text{He}\ ^{23}\text{Na}$	28.98	28.98	28.98	28.98				
$^4\text{He}_2\ ^7\text{Li}$	79.36	45.7	65.6	80.0	73.4	57.1	78.73	50.89
$^4\text{He}_2\ ^6\text{Li}$	57.23	31.4			51.94			35.45
$^4\text{He}_2\ ^{23}\text{Na}$	150.9	103.1	148.5	119.3				

TABLE III. Parameters used in the separable interactions with the corresponding ranges and scattering lengths considered for  $^4\text{He}\ ^7\text{Li}$  (upper part),  $^4\text{He}\ ^6\text{Li}$  (middle part), and  $^4\text{He}\ ^{23}\text{Na}$  (lower part). The references (first columns) are identified in the caption of Table II. For the  $^4\text{He}$  dimer, to fit the binding energy 1.31 mK and corresponding scattering length  $a_{\alpha\alpha} = 100 \text{ \AA}$ , we have  $\gamma_{\alpha\alpha} = 0.39 \text{ \AA}^{-1}$  and  $r_{\alpha\alpha} = 7.34 \text{ \AA}$ .

References	$\gamma_{\alpha\beta} (\text{\AA}^{-1})$	$r_{\alpha\beta} (\text{\AA})$	$a_{\alpha\beta} (\text{\AA})$
$^4\text{He}\ ^7\text{Li}$			
(a1)	0.17	14.77	50.08
(a2)	0.14	19.02	77.43
(a3)	0.144	17.19	51.89
(a4)	0.17	14.68	50.01
(a5)	0.19	13.95	66.10
(a6)	0.16	16.82	67.98
(a7)	0.17	14.72	51.01
(a8)	0.11	21.04	55.02
$^4\text{He}\ ^6\text{Li}$			
(a1)	0.17	15.85	90.38
(a2)	0.14	20.04	300.37
(a5)	0.19	15.11	182.77
(a8)	0.12	22.18	94.40
$^4\text{He}\ ^{23}\text{Na}$			
(a1)	0.16	12.44	25.34
(a2)	0.09	19.0	34.24
(a3)	0.16	12.65	25.58
(a4)	0.11	15.99	29.80

In Table II, we present available two- and three-body ground-state binding energies (absolute values, given in millikelvins), obtained from different realistic potential models (a1)–(a8) for the atomic system we are studying with  $\alpha = ^4\text{He}$ ,  $\beta = ^7\text{Li}$ ,  $^6\text{Li}$ , and  $^{23}\text{Na}$ . Specifically, (a1) is from Ref. [41]; (a2) is from Ref. [18] with interactions from Ref. [44]; (a3) is from Ref. [25] with potentials from Refs. [45,46]; (a4) is from Ref. [25] with potentials from Ref. [47] for  $\alpha\alpha$  and Ref. [46] for  $\alpha\beta$ ; (a5) is from Ref. [24] with potentials from Refs. [48,49]; (a6) is from Ref. [25] with potentials from Ref. [48]; (a7) is from Ref. [27] with potentials from Ref. [49] for  $\alpha\alpha$  and Ref. [46] for  $\alpha\beta$ ; (a8) is from Ref. [28]. These energies are used to adjust the parameters of our zero-range and FR separable interactions.

For the case of FR, the parameters with corresponding ranges and scattering lengths are shown in Table III, given in three blocks for the cases with  $^4\text{He}\ ^7\text{Li}$ ,  $^4\text{He}\ ^6\text{Li}$ , and  $^4\text{He}\ ^{23}\text{Na}$ . We observe that, in all the cases, for the dimer  $^4\text{He}_2$  binding energy, the accepted value of  $B_{\alpha\alpha} = 1.31 \text{ mK}$  is being considered with the corresponding parameters given in the caption of Table III.

### 1. Exploring parameter dependence

In the present paper on scattering observables for the elastic channel of an atom and diatomic molecule collision, we start by presenting some general results when considering that the binding energy for the  $\alpha\beta$  subsystem can be arbitrarily varied, keeping fixed the other two- and three-body binding energies. To explore the general features of this parameter dependence, both in the case of the ZR and in the case of the

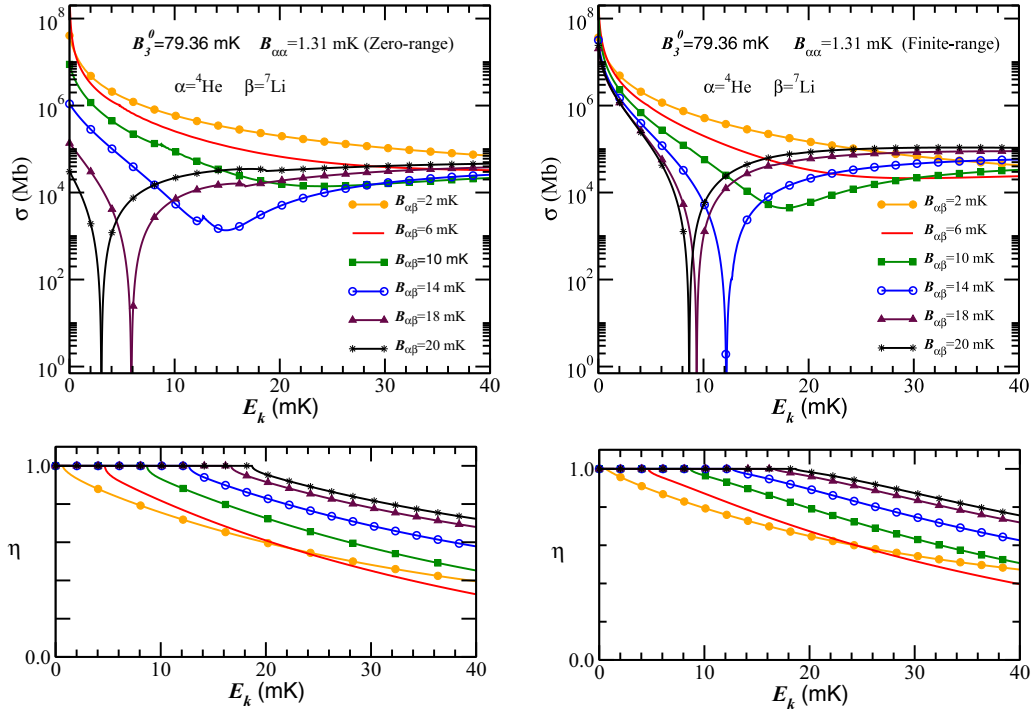


FIG. 2. The  $s$ -wave cross-section  $\sigma$  (upper frames) with the corresponding absorption parameters  $\eta$  (lower frames) for the scattering of  $\alpha \equiv {}^4\text{He}$  by the  $\alpha\beta$  ( ${}^4\text{He}{}^7\text{Li}$ ) system as a function of the kinetic-energy  $E_k$  of the projectile in the center-of-mass system. The results are given by using the zero-range potentials in the left frames and by using the Yamaguchi separable potentials in the right frames. In our parametrization, the binding energies of the subsystem  ${}^4\text{He}_2$  and the three-body ground state are fixed to  $B_{\alpha\alpha} = 1.31$  and  $B_3 = 79.36$  mK, respectively, considering several binding energies for the subsystem  $\alpha\beta$  as given inside the frames.

Yamaguchi models, we use the example of the atom  $\alpha \equiv {}^4\text{He}$  colliding elastically with the dimer ( $\alpha\beta$ ) ( ${}^4\text{He}{}^7\text{Li}$ ). The results, obtained by using zero-range and finite-range one-term separable interactions, are shown for the  $s$ -wave cross sections and corresponding absorption parameters, respectively, in the upper and lower panels of Fig. 2 as functions of the collision energy  $E_k$  in the rest frame.

The comparison between the ZR and the FR results in Fig. 2 shows quite similar results when the two dimer binding energies are comparable such that  $B_{\alpha\beta} \lesssim 5B_{\alpha\alpha}$ . However, as expected the interaction range starts to be more relevant for larger values of  $B_{\alpha\beta}$ . The present results are evidence that, as we increase  $B_{\alpha\beta}$  for a fixed ground-state triatomic molecular binding energy, a minimum starts to emerge in  $\sigma$ , which has the tendency to move towards some value of  $E_k$  as  $B_{\alpha\beta}$  increases. This behavior is quite clear when using finite-range interactions as the range parameters are more relevant to obtain correctly the scattering observables. Possibly such a curious property is due to the less efficient role of the decreasing  $a_{\alpha\beta}$  in cutting the long-range potential as compared to the larger  $a_{\alpha\alpha}$ .

We should also note a cusp in the plots at energies  $E_k = B_{\alpha\beta} - B_{\alpha\alpha}$ , corresponding to the position where the new channel is open. For  $E_k > B_{\alpha\beta} - B_{\alpha\alpha}$ , we verify the effect of the absorption as shown in the lower panels where we note that  $\eta$  tends to saturate with the energy. This is clearly shown in the case for  $B_{\alpha\beta} = 2$  mK, implying that for  $E_k \gg B_{\alpha\beta}$  there is no more possibility to increase the absorption.

The comparison between the results of ZR and Yamaguchi models in Fig. 2 for the  ${}^4\text{He}$  ( ${}^4\text{He}{}^7\text{Li}$ )  $s$ -wave cross section

shows less cases for minima for the ZR calculations. This curious effect can already be thought of as being reasonable because when the effective range is considered  $a_{\alpha\beta}$  increases for a given  $B_{\alpha\beta}$  [cf. Eq. (20)], and therefore there is more room for the logarithmic-periodic behavior of the wave function to establish a zero in  $\delta_0$  for the Yamaguchi potential when compared to the ZR model. Note that the zero turns to a minimum if above the threshold to open the rearrangement channel, which we note by the cusp for energies below the minimum.

The appearance of zeros in the elastic  $s$ -wave cross sections is traced back to the dominance of the logarithmic-periodic behavior of the scattering wave function inside the long-range Efimov potential, extensively discussed in Ref. [38]. Of course as the scattering lengths move to larger values more cycles of the wave function appear in the Efimov potential are possible, allowing for the presence of zeros in the cross sections and the maxima. However, the other side this phenomenon concentrates on small values of the kinetic energies as the opening of a scattering channel tends to wash out these minima as the probability flux is driven to new open channels.

## 2. Realistic ${}^4\text{He}{}^7\text{Li}$ and ${}^4\text{He}{}^6\text{Li}$ parameters

By using different realistic model inputs for the  ${}^4\text{He}{}^7\text{Li}$  and  ${}^4\text{He}{}^6\text{Li}$  dimer binding energies as given in Table II, the results for the cross sections are shown in Fig. 3 in the upper and lower panels, respectively. In both cases, we consider zero-range (left panels) and finite-range (right panels) interactions which are fitting the respective binding energies presented in Table II.

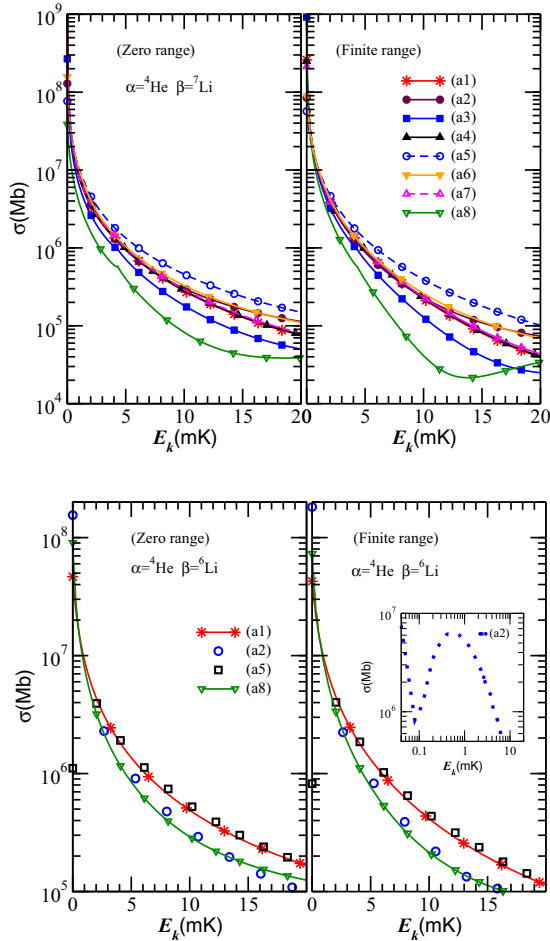


FIG. 3. Results obtained for the  $s$ -wave cross section for the scattering of  ${}^4\text{He}$  from the dimers  ${}^4\text{He}$   ${}^7\text{Li}$  (upper panels) and  ${}^4\text{He}$   ${}^6\text{Li}$  (lower panels). In the left panels we have the results by using zero-range interactions with finite-range results being presented in the right panels. In both cases, we use binding energies obtained from different realistic model calculations as indicated (inside the right upper panel for  $\beta = {}^7\text{Li}$  and inside the left panel for  $\beta = {}^6\text{Li}$ ) with the corresponding references given in the caption of Fig. 1. For model (a2), we also show the results in an inset in the lower-right panel. The finite-range-interaction parameters are given in Table III.

We should observe the characteristic behavior of the plots in Fig. 3 when the collision energy  $E_k$  is very small approaching zero. For the case in which the two-body binding energies for  ${}^4\text{He}$   ${}^6\text{Li}$  are very low as the ones provided by the models from Refs. [18,24] [identified by (a2) and (a5), respectively], we note that each curve of the cross sections is presenting a maximum for  $E_k < 1$  mK. Such behavior can better be understood by scaling all the energies ( $E_k$  and the two-body binding energies) using the corresponding three-body ground-state energies as was performed in Ref. [38]. As learned from the studies for atom-molecule collision at very low energies performed in Ref. [38] when considering small enough values for the subsystem binding as  $E_k$  is decreased, one should observe maxima and minima in the corresponding  $s$ -wave cross section.

This behavior can be seen in the two cases that we use as input dimer energies  $B_{\alpha\beta}$  that are very low in comparison

with the three-body ground-state energies. Indeed, when the two-body energy is close to the unitary limit, the cross section should present a series of maxima and minima for enough small values of  $E_k$  in the limit that the mass ratio  $m_\alpha/m_\beta$  becomes very small with similar behavior as the Efimov excited states (see Ref. [38]). However, in our present case, no more than one maximum is observed in each curve because the mass ratios are not as small as the ones considered in Ref. [38]. Therefore, the curious behavior observed in the two plots shown in the lower panels of Fig. 3 (when using  ${}^6\text{Li}$ ) is a manifestation of the same singular behavior for the scattering function  $k \cot \delta_0$ , known for a long time from neutron-deuteron studies [50] and recently studied in Ref. [38].

We call the reader's attention to the minimum in the cross section produced by the input parameters of model (a2) with the Yamaguchi potential in the case of the elastic collision of  ${}^4\text{He}$  on the  ${}^4\text{He}$   ${}^6\text{Li}$  molecule as shown in the inset in the lower panel of Fig. 3. As verified in Ref. [38], when going to a limit with very small two-body binding, at some specific energies the scattering observable  $k \cot \delta_0$  turns out to be singular, leading to zeros in the corresponding cross section. The zero will happen if there is no absorption, which is the case for  $E_k < B_{\alpha\beta} - B_{\alpha\alpha}$ . However, in the present case of model (a2),  $B_{\alpha\beta} - B_{\alpha\alpha} < 0$  such that  $E_k$  can never be less than zero. As absorption is always possible, instead of a zero we observe a minimum in the  $s$ -wave cross section, which follows from Eq. (19),

$$\sigma = \pi \frac{|\eta e^{2i\delta_0} - 1|^2}{k^2}, \quad (21)$$

such that  $\sigma = \pi |\eta - 1|^2/k^2$  for  $\delta_0 = 0$ , characterizing a minimum instead of a zero when  $\eta \neq 1$ . A similar behavior can be seen with the results for  $\sigma$  given by model (a5). However, as in this case  $B_{\alpha\beta} = 0.33$  mK is not as small as the value we have from model (a2), and the minimum is not clearly characterized in the results of Fig. 3 but evidenced by a point very close to  $E_k = 0$  (see in both lower panels of Fig. 3 the results represented by the black squares). About the possible observation of a zero or minimum in the  $s$ -wave cross section for the scattering of  ${}^4\text{He}$  in  ${}^4\text{He}$   ${}^6\text{Li}$ , it should be disregarded as not being expected from more recent realistic calculations identified by (a1) and (a8) (from Refs. [28,41], respectively).

For the case of the  ${}^4\text{He}$   ${}^7\text{Li}$  molecule as shown in the upper panels of Fig. 3 with different models, most of the results for the cross section have similar behaviors, considering that the energies  $B_{\alpha\beta}$  are not so low in comparison with the three-body ones. Model (a8), given by Ref. [28], which is showing a minimum in the cross section for  $E_k$  near 13 mK, is indicating the minimum of the cross sections for higher collision energies as the ratio  $B_{\alpha\beta}/B_3^{(0)}$  is increased as already discussed when exploring the cross section for different inputs in Fig. 2. Among the models considered with  ${}^7\text{Li}$ , (a8) is the one which provides the larger value for the ratio  $B_{\alpha\beta}/B_3^{(0)}$ . As a general remark, we note that the curves for the cross sections for  $E_k \lesssim 15$  mK follow the energy ratios  $B_{\alpha\beta}/B_3^{(0)}$  with the curves in the upper part being the ones with smaller values for this ratio.

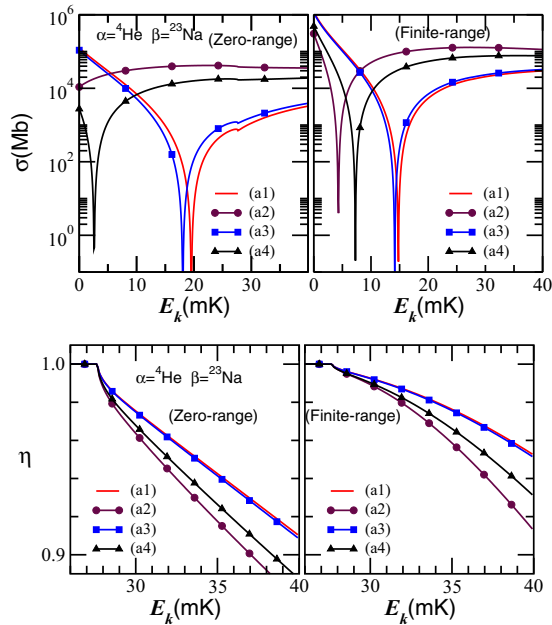


FIG. 4. Cross-section  $\sigma$  (upper panels) and absorption parameter  $\eta$  (lower panels)  $s$ -wave results for the collision of  ${}^4\text{He}$  in the  ${}^4\text{He}{}^{23}\text{Na}$  dimer. The two- and three-body energies used in the calculations are indicated inside the panels, being given by models quoted in the caption of Table II. The zero-range results are in the left frames with the finite-range separable Yamaguchi results shown in the right frames.

### C. Zero of ${}^4\text{He}({}^4\text{He}{}^{23}\text{Na})$ $s$ -wave cross section

In the case of the scattering of  ${}^4\text{He}$  by the  ${}^4\text{He}{}^{23}\text{Na}$  molecule with four different realistic model calculations available, our results are shown in Fig. 4 for the cross sections (upper frames) and absorption parameters (lower frames).

We observe the same general features of the elastic  $s$ -wave cross section already pointed out by the results shown in Fig. 2, namely, with the increase in the binding energy of the subsystem  $\alpha\beta$  a minimum emerges at some value of  $E_k$ . As  $B_{\alpha\beta}$  increases, the tendency of this minimum seems to converge to some value of  $E_k$ . This can be seen by matching the binding energies given for  ${}^4\text{He}{}^{23}\text{Na}$  in the last line of Table II with the minima appearing in Fig. 4 when considering finite-range results. Also, as noted in the case of Fig. 2, the convergence of the minima to some value  $E_k$  when using the ZR results is not so fast and clear as in the case with the FR results.

More relevant to eventually future scattering experiments of the  ${}^4\text{He}$  collision with the  ${}^4\text{He}{}^{23}\text{Na}$  molecule is our conclusion of a minimum in the elastic  $s$ -wave cross section from finite-range interactions within our approach and using different realistic model calculations as inputs. Considering the more recent realistic model calculations (a1) reported in Ref. [41], a minimum should occur in the cross section at a center-of-mass collision energy close to  $E_k \sim 15$  mK. This prediction seems robust as the ZR model with the same input predicts the position of the zero around 20 mK.

## IV. CONCLUSION

We predict the  $s$ -wave scattering properties of cold  ${}^4\text{He}$  elastic collision with the  ${}^4\text{He}{}^{6,7}\text{Li}$  and  ${}^4\text{He}{}^{23}\text{Na}$  molecules for center-of-mass kinetic energies up to 40 mK. Of particular experimental relevance, considering the actual investigations in cold atom laboratories, we show the presence of a minimum in the  $s$ -wave elastic cross section for the  ${}^4\text{He} \rightarrow ({}^4\text{He}{}^{23}\text{Na})$  scattering. This prediction was based on calculations performed using finite-range separable interactions where we used recent realistic model results for the molecular bound-state energies as inputs to get the model parameters. By using the binding energies reported in Ref. [41], we predict that the elastic  $s$ -wave cross section should have a minimum at a center-of-mass colliding energy close to  $E_k \sim 15$  mK. In our approach, we have also obtained the corresponding  $s$ -wave absorption parameter, which is relevant for defining the  $s$ -wave scattering amplitude.

To access the importance of the range corrections to the phase shifts and absorption parameters, our calculations were performed with the zero-range model and a finite-range one-term separable potential. The results present some sensitivity to the potential range when the binding energies for the two-body subsystems are not low enough with respect to the three-body ground-state energy. It is well known that close to the Efimov limit, namely, zero dimer binding energies, the low-energy three-body observables are model independent and dominated by few low-energy scales as in our case with the diatomic and ground-state triatomic binding energies.

The model independence is exemplified in this paper with universal scaling plots, considering the correlation of the excited-state energy of  ${}^4\text{He}_2{}^{6,7}\text{Li}$  with the  ${}^4\text{He}{}^{6,7}\text{Li}$  molecule binding. Such correlations are pronounced close to the unitary limit, however, our examples of cold collisions are not at the unitarity taking into account the realistic potential model results for the binding energies of the di- and triatomic molecules and atom-atom scattering lengths. Despite that we have shown that, although the elastic  $s$ -wave cross section presents some sensitivity on the potential range the basic universal predictions are not destroyed, such as the robust presence of the zero in the elastic  $s$ -wave cross section of  ${}^4\text{He}$  on the  ${}^4\text{He}{}^{23}\text{Na}$  molecule, which we expect to motivate the experimentalist to observe such a property at the root of the universal Efimov physics.

Finally, we should mention some perspectives on further related investigations. First, as stated in the Introduction, a direct extension of this paper is to explore the contribution of higher partial waves in the total cross section, which is expected to be non-negligible as we move to higher energies. Also relevant, in our understanding, are the possible inelastic processes in the atom-dimer  $\alpha \rightarrow (\alpha\beta)$  collision, such as three-body rearrangements going to  $(\alpha\alpha) + \beta$  or total dissociation  $(\alpha + \alpha + \beta)$ ; processes expected to be significant at the collision energies we have used, deserving a separate detailed investigation.

## ACKNOWLEDGMENTS

This work was partially supported by Fundação de Amparo à Pesquisa do Estado de São Paulo (Grant No. 17/05660-0),

Coordenação de Aperfeiçoamento de Pessoal de Nível Superior, Conselho Nacional de Desenvolvimento Científico

e Tecnológico and Project INCT-FNA (CNPq Grant No. 464898/2014-5).

- [1] V. Efimov, *Phys. Lett. B* **33**, 563 (1970); *Nucl. Phys. A* **362**, 45 (1981); *Comments Nucl. Part. Phys.* **19**, 271 (1990).
- [2] S. K. Adhikari, A. Delfino, T. Frederico, I. D. Goldman, and L. Tomio, *Phys. Rev. A* **37**, 3666 (1988).
- [3] L. H. Thomas, *Phys. Rev.* **47**, 903 (1935).
- [4] S. K. Adhikari and L. Tomio, *Phys. Rev. C* **26**, 83 (1982).
- [5] I. Tanihata, *J. Phys. G: Nucl. Part. Phys.* **22**, 157 (1996).
- [6] D. V. Fedorov and A. S. Jensen, *Phys. Rev. Lett.* **71**, 4103 (1993); D. V. Fedorov, A. S. Jensen, and K. Riisager, *ibid.* **73**, 2817 (1994); D. V. Fedorov, E. Garrido, and A. S. Jensen, *Phys. Rev. C* **51**, 3052 (1995); P. G. Hansen, A. S. Jensen, and B. Jonson, *Annu. Rev. Nucl. Part. Sci.* **45**, 591 (1995).
- [7] S. Dasgupta, I. Mazumdar, and V. S. Bhasin, *Phys. Rev. C* **50**, R550 (1994).
- [8] A. E. A. Amorim, T. Frederico, and L. Tomio, *Phys. Rev. C* **56**, 2378(R) (1997).
- [9] P. F. Bedaque and U. van Kolck, *Ann. Rev. Nucl. Part. Sci.* **52**, 339 (2002).
- [10] E. Braaten and H.-W. Hammer, *Phys. Rep.* **428**, 259 (2006).
- [11] E. Epelbaum, H.-W. Hammer, and U.-G. Meißner, *Rev. Mod. Phys.* **81**, 1773 (2009).
- [12] T. Frederico, A. Delfino, L. Tomio, and M. T. Yamashita, *Prog. Part. Nucl. Phys.* **67**, 939 (2012).
- [13] H.-W. Hammer, C. Ji, and D. R. Phillips, *J. Phys. G: Nucl. Part. Phys.* **44**, 103002 (2017).
- [14] T. K. Lim, K. Duffy, and W. C. Damert, *Phys. Rev. Lett.* **38**, 341 (1977).
- [15] H. S. Huber and T. K. Lim, *J. Chem. Phys.* **68**, 1006 (1978); H. S. Huber, T. K. Lim, and D. H. Feng, *Phys. Rev. C* **18**, 1534 (1978).
- [16] S. Nakaichi-Maeda and T. K. Lim, *Phys. Rev. A* **28**, 692 (1983).
- [17] T. Cornelius and W. Glöckle, *J. Chem. Phys.* **85**, 3906 (1986).
- [18] J. Yuan and C. D. Lin, *J. Phys. B: At., Mol. Opt. Phys.* **31**, L637 (1998).
- [19] T. Frederico, L. Tomio, A. Delfino, and A. E. A. Amorim, *Phys. Rev. A* **60**, 9(R) (1999).
- [20] S. Huber, *Phys. Rev. A* **31**, 3981 (1985).
- [21] B. D. Esry, C. D. Lin, and C. H. Greene, *Phys. Rev. A* **54**, 394 (1996).
- [22] E. A. Kolganova, A. K. Motovilov, and S. A. Sofianos, *Phys. Rev. A* **56**, 1686(R) (1997); A. K. Motovilov, W. Sandhas, S. A. Sofianos, and E. A. Kolganova, *Eur. Phys. J. D* **13**, 33 (2001); E. A. Kolganova, A. K. Motovilov, and W. Sandhas, *Phys. Rev. A* **70**, 052711 (2004).
- [23] A. Delfino, T. Frederico, and L. Tomio, *J. Chem. Phys.* **113**, 7874 (2000).
- [24] I. Baccarelli, G. Delgado-Barrio, F. A. Gianturco, T. Gonzalez-Lezana, S. Miret-Artés, and P. Villarreal, *Europhys. Lett.* **50**, 567 (2000).
- [25] C. Di Paola, F. A. Gianturco, F. Paesani, G. Delgado-Barrio, S. Miret-Artés, P. Villarreal, I. Baccarelli, and T. González-Lezana, *J. Phys. B: At., Mol. Opt. Phys.* **35**, 2643 (2002).
- [26] V. Roudnev and M. Cavagnero, *J. Phys. B: At., Mol. Opt. Phys.* **45**, 025101 (2012).
- [27] M.-S. Wu, H.-L. Han, C.-B. Li, and T.-Y. Shi, *Phys. Rev. A* **90**, 062506 (2014).
- [28] E. A. Kolganova, *Few-Body Syst.* **58**, 57 (2017); **59**, 28 (2018).
- [29] R. E. Grisenti, W. Schöllkopf, J. P. Toennies, G. C. Hegerfeldt, T. Köhler, and M. Stoll, *Phys. Rev. Lett.* **85**, 2284 (2000).
- [30] M. Kunitski *et al.*, *Science* **348**, 551 (2015).
- [31] M. Zaccanti, B. Deissler, C. D'Errico, M. Fattori, M. Jonas-Lasinio, S. Müller, G. Roati, M. Inguscio, and G. Modugno, *Nat. Phys.* **5**, 586 (2009); S. E. Pollack, D. Dries, and R. G. Hulet, *Science* **326**, 1683 (2009); F. Ferlaino, S. Knoop, M. Berninger, W. Harm, J. P. D'Incao, H.-C. Nägerl, and R. Grimm, *Phys. Rev. Lett.* **102**, 140401 (2009); S. Knoop, F. Ferlaino, M. Mark, M. Berninger, H. Schöbel, H.-C. Nägerl, and R. Grimm, *Nat. Phys.* **5**, 227 (2009).
- [32] G. Barontini, C. Weber, F. Rabatti, J. Catani, G. Thalhammer, M. Inguscio, and F. Minardi, *Phys. Rev. Lett.* **103**, 043201 (2009); **104**, 059901(E) (2010); R. S. Bloom, M.-G. Hu, T. D. Cumby, and D. S. Jin, *ibid.* **111**, 105301 (2013); R. Pires, J. Ulmanis, S. Häfner, M. Repp, A. Arias, E. D. Kuhnle, and M. Weidemüller, *ibid.* **112**, 250404 (2014); J. Ulmanis, S. Häfner, E. D. Kuhnle, and M. Weidemüller, *Natl. Sci. Rev.* **3**, 174 (2016).
- [33] F. Bringas, M. T. Yamashita, and T. Frederico, *Phys. Rev. A* **69**, 040702 (2004).
- [34] Y. Wang, J. P. D'Incao, H.-C. Nägerl, and B. D. Esry, *Phys. Rev. Lett.* **104**, 113201 (2010).
- [35] J. Levensen and D. S. Petrov, *Eur. Phys. J. D* **65**, 67 (2011).
- [36] E. Garrido, C. Romero-Redondo, A. Kievsky, and M. Viviani, *Phys. Rev. A* **86**, 052709 (2012).
- [37] D. Blume and Y. Yan, *Phys. Rev. Lett.* **113**, 213201 (2014).
- [38] M. A. Shalchi, M. T. Yamashita, M. R. Hadizadeh, E. Garrido, L. Tomio, and T. Frederico, *Phys. Rev. A* **97**, 012701 (2018).
- [39] S. Inouye, M. R. Andrews, J. Stenger, H.-J. Miesner, D. M. Stamper-Kurn, and W. Ketterle, *Nature (London)* **392**, 151 (1998); E. Timmermans, P. Tommasini, M. Hussein, and A. Kerman, *Phys. Rep.* **315**, 199 (1999).
- [40] A. Gammal, T. Frederico, L. Tomio, and P. Chomaz, *Phys. Rev. A* **61**, 051602(R) (2000); A. Gammal, T. Frederico, and L. Tomio, *Phys. Rev. E* **60**, 2421 (1999).
- [41] H. Suno, *Phys. Rev. A* **96**, 012508 (2017).
- [42] M. A. Shalchi, M. T. Yamashita, M. R. Hadizadeh, T. Frederico, and L. Tomio, *Phys. Lett. B* **764**, 196 (2017).
- [43] P. F. Bedaque, H.-W. Hammer, and U. van Kolck, *Phys. Rev. Lett.* **82**, 463 (1999).
- [44] U. Kleinekathöfer, K. Tang, J. Toennies, and C. Yiu, *Chem. Phys. Lett.* **249**, 257 (1996).
- [45] U. Kleinekathöfer, K. T. Tang, J. P. Toennies, and C. L. Yiu, *J. Chem. Phys.* **107**, 9502 (1997).
- [46] U. Kleinekathöfer, M. Lewerenz, and M. Mladenović, *Phys. Rev. Lett.* **83**, 4717 (1999).
- [47] K. T. Tang, J. P. Toennies, and C. L. Yiu, *Phys. Rev. Lett.* **74**, 1546 (1995).
- [48] D. Cvetko, A. Lausi, A. Morgante, F. Tommasini, P. Cortona, and M. G. Dondi, *J. Chem. Phys.* **100**, 2052 (1994).
- [49] R. A. Aziz and M. J. Slaman, *J. Chem. Phys.* **94**, 8047 (1991).
- [50] J. S. Whiting and M. G. Fuda, *Phys. Rev. C* **14**, 18 (1976); B. A. Girard and M. G. Fuda, *ibid.* **19**, 579 (1979).